




Cite this: DOI: 10.1039/d6ce00269b

 Received 5th April 2026,
Accepted 30th April 2026

DOI: 10.1039/d6ce00269b

rsc.li/crystengcomm

Weak interactions in metallo-supramolecular grid crystals: an analysis of their effects†

 Jack Harrowfield,^{*a} Juan Ramirez^{abc} and Adrian-Mihail Stadler ^{*abc}

The technique of Hirshfeld surface analysis has been applied to a selection of crystal structures of metallo-supramolecular grids in order to better define the modes of interaction of the grids with both anionic and neutral species, and to assess the possibilities of using grids as selective receptors. The influence of weak interactions on grid symmetry and hence inequivalence of metal sites within the grids has also been considered as a factor influencing possible electronic uses of grid species.

Introduction

Important examples of the designed organisation of complex matter¹ are the regular two-dimensional arrays of metal ions linked by polytopic ligands L which constitute the family of metallogrids.^{2–9} Most easily prepared and thus most common are those of M₄L₄ composition termed [2 × 2] grids, where M is very often a dipositive transition metal ion and L a ditopic, functionalised aromatic ligand, although a great variety of other compositions, including those of the general formula [m × n] where m ≠ n and those of heterometallic species, are also well known.^{2–9} Where L is a neutral species, counter anions must of course be associated with the grid. Such compositional variations are associated with widely different electronic, magnetic and optical properties,^{10–12} offering in many cases potential applications, for example, in molecular electronics^{13–15} or biochemistry.¹⁶ A large family of [2 × 2] grids (Fig. 1(a)) has been developed through the rational design of ditopic ligands (based, in many instances, on a pyrimidine-bridge core) and the eventual use (*e.g.*¹⁷) of template¹⁸ or “sub-component assembly”¹⁹ metal-ion-assisted Schiff base formation reactions to avoid the necessity of first assembling the free ligand. Characterisation of this family has produced a significant volume of single-crystal, X-ray structural data not only of value in establishing the grid form in detail but potentially also in defining the weak interactions²⁰ of the grid units in the solid state. In principle, these interactions may involve both the internal cavity of the

grid unit itself and spaces within the array of grids forming the crystal, the former being a site of dimensions determined by those of the ditopic ligands and thus open to controlled variation. Obvious questions to be asked in relation to this are: (i) in cationic grids, can both (counter) anionic and neutral species be located within the cavities of these grids? (ii) Can weak interactions between the grid and neutral or anionic species give rise to selectivity in their binding?

Answers to these questions are interesting not only from a theoretical point of view but also for the design of devices for the capture and transport of anions or small neutral molecules, anion binding in solution being well established²¹ and indeed known to determine whether or not a grid is formed,^{22,23} while recent work has shown that [2 × 2] Ni(II) grids, for example, can be used as solid state CO₂ sensors.²⁴ Of possibly greater significance is the fact that metallogrids are one group of species of potential interest in the search for paramagnetic metal ion based “qubits”.^{25,26} Here, it is especially important to know how the metal ion coordination environment may vary in different grid species.

While the adjective “weak” implies that interactions of this type do not have a major influence on structure, it may be noted that a change in an equilibrium or rate constant by a factor of 100 corresponds to a change in free or activation energy by about 10 kJ mol^{−1}, a change which lies near the mean of the strength of a variety of “weak interactions”.^{20,27} Thus, their influence is unlikely to be negligible on both structure and reactivity. One particularly useful means of characterising weak interactions exceeding dispersion in crystalline solids is through the evaluation of Hirshfeld surfaces²⁸ as described in the program CrystalExplorer.²⁹ To do so in detail means that ideally the structure concerned must be one of high quality, free of problems such as disorder, partial occupancy or lack of chemical identification of some portion of the total electron density. This is rather rarely the case, especially if the location of all hydrogen atoms is included as a criterion but useful conclusions may

^a Institut de Science et d'Ingénierie Supramoléculaires (ISIS), CNRS – Université de Strasbourg, UMR 7006, 8 Allée Gaspard Monge, 67000 Strasbourg, France.

E-mail: jacmacbharr@gmail.com, mstadler@unistra.fr

^b University of Strasbourg Institute for Advanced Study (USIAS), 5 Allée du Général Rouvillois, 67083 Strasbourg, France

^c Institut für Nanotechnologie (INT), Karlsruhe Institut für Technologie (KIT), 76344 Eggenstein-Leopoldshafen, Germany

† Dedicated to Professor Jean-Marie Lehn on the occasion of the 60th anniversary (in 2025) of the founding of his research group.



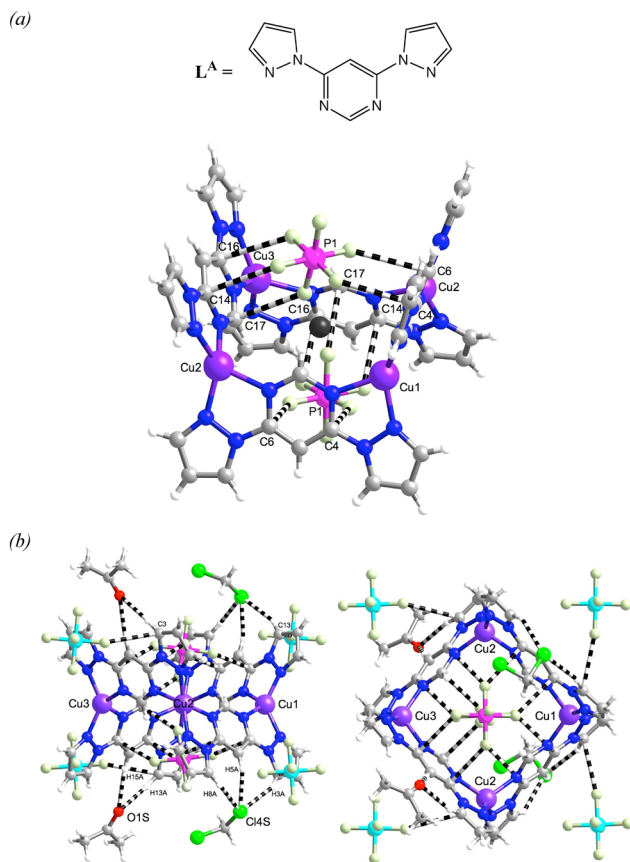


Fig. 1 (a) A perspective view of the grid unit present in the crystal²¹ of $[\text{Cu}_4(\text{L}^{\text{A}})_4](\text{PF}_6)_4 \cdot 2(\text{CH}_3)_2\text{CO} \cdot 2\text{CH}_2\text{Cl}_2$ showing the two included hexafluorophosphate anions and their interactions (dashed lines) with pyrimidine C-atoms. The centroid of the Cu_4 unit is shown as a black sphere to indicate that the anions do not penetrate far into the central cavity. F-atoms (pale green) involved in the interactions are numbered in the text. (b) Orthogonal views of the grid showing the complete set of weak interactions involving anions and solvents, emphasising the twofold rotational symmetry of the aggregate. To limit congestion, atom numbers are shown for only one set of symmetry-related atoms. P-atoms of the peripherally bonded anions are shown in light blue, those included, in pink.

nonetheless be drawn even where satisfaction of these criteria is limited. This we illustrate here by consideration of a selection of structures of $[2 \times 2]$ (M_4L_4) grids derived mostly from pyrimidine-core ligands. For simplicity, we consider mainly ditopic ligands where the two metal ion binding sites are identical. Such ligands generate “classical” grids, where both coordination sites of each bound ditopic ligand adopt the same orientation.³⁰ For the sake of clarity and simplicity, in the structural formulae of ligands L^{A} to L^{M} and in that of ligand L^{P} , the conformation of the heterocyclic part is represented as found in grids, while the structural formulae of ligands L^{N} and L^{O} show conformations of the heterocyclic part which correspond partly to those observed in grids.

Discussion

The first $[2 \times 2]$ metallogrid to be structurally characterised (CCDC 1190310; refcode JUGBES),³¹ though not a complex of

a pyrimidine-derived ligand, defined features found in the majority of presently known metallogrids in that while its solution ^1H NMR spectrum was consistent with all four metal ion centres ($\text{Cu}(\text{I})$) being equivalent, this was not the case in the crystal, and in that as a cationic species it was accompanied in its crystal form by not only counteranions but by solvent. Later work²¹ on two pyrimidine-derived ditopic ligands similarly designed to be suited to metal ions favouring tetrahedral coordination involved X-ray structural characterisation of three $\text{Cu}(\text{I})$ complexes, two of the structures satisfying all of the criteria given above for full present analysis of the Hirshfeld surfaces. The most informative of these was the structure of $[\text{Cu}_4(\text{L}^{\text{A}})_4](\text{PF}_6)_4 \cdot 2(\text{CH}_3)_2\text{CO} \cdot 2\text{CH}_2\text{Cl}_2$ (L^{A} = 4,6-bis(pyrazol-1-yl)pyrimidine; Fig. 1; CCDC 162905; refcode TIWCOS), analysed in some detail originally,²¹ though with a focus on the grid-anion interactions, and consideration of the Hirshfeld surface offers further refinements. (Details of this procedure for all the currently considered species are given in the SI.) Thus, although neither hexafluorophosphate anions nor solvent molecules actually cross the mean plane of the four $\text{Cu}(\text{I})$ ions, one anion lies above each face of this plane and two anions can therefore be considered to be included by the grid core. Originally²¹ described just as anion $\cdots\pi$ interactions adding to electrostatic attraction, the Hirshfeld surface indicates that these interactions are mediated by short $\text{F}\cdots\text{C}(\text{pyrimidine})$ contacts $\text{C4}\cdots\text{F10}$ 2.96; $\text{C6}\cdots\text{F9}$ 2.96; $\text{C14}\cdots\text{F12}$ 3.08; $\text{C16}\cdots\text{F11}$ 3.07 and $\text{C17}\cdots\text{F2}$ 3.05 Å (Fig. 1(a); for clarity in visualising the weak interactions, shown as dashed lines, in this and all other figures, atom numbering is limited but details, including atom separations, can be found in the SI, section 2. In general, unless otherwise noted, atom colours are H white, B dark green, C grey, N dark blue, O red, F pale green, P violet, S orange, Cl clear green.). These bridge opposed pyrimidine units of the grid in an unsymmetrical manner, C4 and C6 belonging to one and C14, C16 and C17 to the other, and this may explain why the ligand mean planes are inclined at angles of 114 and 115° to the Cu_4 mean plane (defined as the angle between the centroid of the Cu_4 unit, C1 and C4 atoms of the pyrimidine rings). The grid is further distorted by interactions with both solvent species, although these interactions do not involve inclusion within the cavity defined by the Cu_4L_4 unit. Unlike the included-anion-grid interactions, those of the solvent molecules involve O (acetone) or Cl (dichloromethane) contacts with CH atoms of both the pyrimidine and pyrazolyl units of the ligand ($\text{O1S}\cdots\text{H15A}$ 2.36, $\text{O1S}\cdots\text{H13A}$ 2.41 Å; $\text{Cl4S}\cdots\text{H3A}$ 2.56, $\text{Cl4S}\cdots\text{H5O}$ 2.30, $\text{Cl4S}\cdots\text{H8A}$ 2.62 Å) and are such as to reinforce the local C_2 symmetry of the grid about the Cu1–Cu3 axis associated with the included anion interactions (Fig. 1(b)). This symmetry is also seen in $\text{F}\cdots\text{C}(\text{pyrazolyl})$ interactions ($\text{F6}\cdots\text{C3}$ 3.02; $\text{F7}\cdots\text{C13}$ 3.10 Å) involving the unincluded anions that serve, along with dispersion forces and barely discernible further interactions exceeding dispersion of the solvent molecules, to assemble grid units within the full crystal structure.



Use of tetrafluoroborate rather than hexafluorophosphate to crystallise $[\text{Cu}_4(\text{L}^{\text{A}})_4]^{4+}$ provided an unsolvated crystal²¹ (Fig. 2(a); CCDC 681835; refcode TIWCUY) but also one involving partial disorder of the anions. Two ordered anions were again found included in the grid cavity but here they were inequivalent and the Hirshfeld surface indicates that their interactions with the grid involve both pyrimidine- $\text{CH}\cdots\text{F}$ and pyrimidine- $\text{C}\cdots\text{F}$ contacts but in different ways (Fig. 2(a)). $[\text{BF}_4]^-$ is of course a considerably smaller anion than $[\text{PF}_6]^-$, so different modes of inclusion may be anticipated and here the consequences are that the weak interactions create an aggregate with one plane of symmetry, meaning that there are now only two inequivalent Cu(i) centres within the grid, with opposed pairs of ligand units making quite different angles of 108 and 133° with the Cu_4 mean plane. Disorder of the uninvolved anions renders interpretation of their interactions speculative.

More precise information on $[\text{BF}_4]^-$ interactions with a grid (formed from a ligand closely related to L^{A}) can, however, be obtained from the reported²¹ structure of the ordered, unsolvated grid $[\text{Cu}_4(\text{L}^{\text{B}})_4](\text{BF}_4)_4$ (Fig. 2(b); CCDC 681836; refcode TIWDAF), where L^{B} is the tetramethylated derivative of L^{A} , 4,6-bis(3,5-dimethylpyrazol-1-yl)pyrimidine. Here again, two anions are held in close proximity to the Cu_4 mean plane and can be considered included in the grid cavity through both pyrimidine- $\text{CH}\cdots\text{F}$ and pyrimidine- $\text{C}\cdots\text{F}$ interactions but in this case the two anions are equivalent and are related by a twofold rotation axis, explaining the presence of two inequivalent Cu(i) centres in each grid unit (Fig. 2(b)). All opposed ligand units are tilted slightly away from one another, with a tilt angle of 111.7° towards the Cu_4 plane. The uninvolved anions are involved in methyl- $\text{CH}\cdots\text{F}$ interactions which bridge grid units.

Worthy of note is that reference 21 also describes the crystal structures of two unsolvated complexes involving the

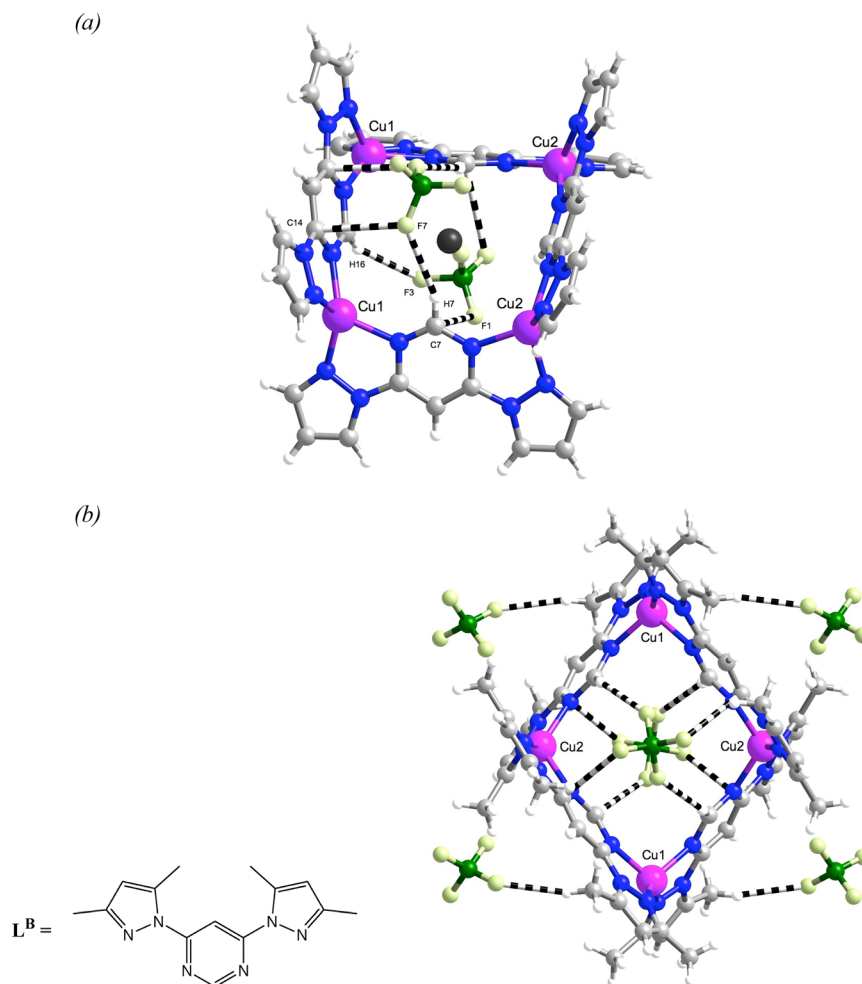


Fig. 2 (a) The grid and two included tetrafluoroborate anions found in the crystal structure²¹ of unsolvated $[\text{Cu}_4(\text{L}^{\text{A}})_4](\text{BF}_4)_4$, again shown with partial atom numbering of one set of symmetry related atoms involved in weak interactions ($\text{F1}\cdots\text{C7}$ 3.08, $\text{F3}\cdots\text{H16}$ 2.39, $\text{F7}\cdots\text{C14}$ 3.01, $\text{F7}\cdots\text{H7}$ 2.58 Å). One anion is much closer to the centroid (black sphere) of the Cu_4 unit than the other but the whole array has a plane of symmetry. (b) Weak interactions of the grid in the crystal²¹ of unsolvated $[\text{Cu}_4(\text{L}^{\text{B}})_4](\text{BF}_4)_4$ which produce an aggregate with two fold rotational symmetry. Atom separations: $\text{F}\cdots\text{C}$ (pyrimidine) 3.03, $\text{F}\cdots\text{H}$ (pyrimidine) 2.43, $\text{F}\cdots\text{H}$ (methyl) 2.49 Å.



$[\text{Cu}_4(\text{L}^{\text{C}})_4]^{4+}$ cation, where $\text{L}^{\text{C}} = 3,6\text{-bis}(3,5\text{-dimethylpyrazol-1-yl})\text{pyridazine}$ (Fig. 3), in association with hexafluorophosphate or tosylate (4-methylbenzenesulfonate) anions (CCDC 681837 and 681838; refcodes TIWDEJ and TIWDIN). The intention there was to investigate the effects of changing the relative orientation of the two metal ion binding sites of the ligand, an issue relevant to the nature of pyrimidine-core ligands discussed ahead, but a prominent effect of the use of a pyridazine bridge unit was the reduction of the grid dimensions from a $\text{Cu}\cdots\text{Cu}$ side length of ~ 6.1 to ~ 3.6 Å, removing any possibility of anion inclusion and leading to complicated arrays of cation–anion interactions causing all four Cu centres to be inequivalent (Fig. 3).

The construction of ditopic ligands suitable for formation of grids based on octahedral coordination has in general led to more complicated superstructures than those of the ligands just discussed, one useful consequence being the greater variety of chemistry to be found, such as through ligand deprotonation reactions.^{3,5–8,17,32} Retention of a pyrimidine core in the ligand design does of course limit the grid side length in octahedral metal ion grids to values similar to those of the tetrahedral metal ion grids described above but this does mean that inclusion of small anions is clearly possible. It is in fact rather unclear what criteria other than those given above for small anion inclusion should be applied to the possible occupancy of central grid cavities, since the only established example (CCDC 123202; refcode RUHXUN; a Cu_4 grid structure) of true inclusion of a small molecule (benzene)³³ is that where the grid side length is rather long at ~ 7.7 Å and this binding is attributed to aromatic π – π interactions, while the formation of the remarkable Co(II)/Co(III) grid catenane $[\text{Co}_4(\text{pttp})_4]_2[\text{Co}(\text{NCS})_4]_2(\text{NCS})_4 \cdot 8\text{CH}_3\text{OH} \cdot 11\text{H}_2\text{O}$ (ref. 34) (CCDC 279772; refcode MAYXEQ; pttp = dianion of 2-pyridyl amidrazone of oxalyldihydrazide) shows that complete penetration of the grid cavity is possible where the mean grid side length is nearly 1 Å shorter. In the latter case, it has been argued³⁴ that while aromatic π – π interactions are probably

important in stabilising the structure, so too is H-bonding. Neither of these grids involves a pyrimidine core ligand but the early discovery³⁵ that a 2-phenylpyrimidine rather than an unsubstituted pyrimidine core in bis(tridentate) ligands produced grids of greater stability was rationalised in terms of stacking interactions of the phenyl substituents which severely restrict the actual free space at the centre of the grid. Thus, of the large number of $[2 \times 2]$ grids formed by ligands with a 2-phenylpyrimidine core, it is unsurprising to find that only one, $[\text{Fe}_4(\text{L}^{\text{D}})_4]\text{Cl}(\text{ClO}_4)_7 \cdot 7\text{CH}_3\text{NO}_2 \cdot 6\text{H}_2\text{O}$ (Fig. 4; CCDC 238750; refcode FEKRET),³⁶ includes a guest close to the centre of its M_4 unit and that this guest is chloride ion. Unfortunately, the disorder in this somewhat complicated structure renders proper interpretation of the Hirshfeld surface uncertain but it can be said that the included chloride is within 2.7 Å of a tetrahedral array of hydrogen atoms of the phenyl substituents while two perchlorate anions are partially enclosed in sections of the grids between the corners, with O-contacts to aromatic–CH atoms near 2.6 Å (while two others held in similar positions appear to be held by dispersion only). This array of interactions gives the grid aggregate twofold rotational symmetry about an axis perpendicular to the mean metal ion (Fe(II)) plane passing through the chloride, so that there are two inequivalent metal ion centres (Fig. 4).

The complicated nature of the balance achieved between several weak interactions is illustrated in the fact that, perhaps surprisingly, the lack of a 2-phenyl substituent on the pyrimidine core of bis(tridentate) ligands does not seem to guarantee inclusion of small species within the M_4 ring of derived grids. In the crystal structure of the complex $[\text{Fe}_2\text{Ru}_2(\text{L}^{\text{E}})_4]\text{Cl}_2(\text{PF}_6)_2 \cdot 3\text{CH}_3\text{CN}$ (Fig. 5(a); CCDC 101633; refcode SIQPIR),³⁷ unfortunately again one where disorder is extensive, one chloride ion occupies a position similar but not identical to that in FEKRET (Fig. 4), while another lies in a position which might be considered as a cap to the internal cavity but is remote from the Fe_2Ru_2 mean plane. The latter position is better defined in the structure of $[\text{Fe}_4(\text{L}^{\text{F}})_4](\text{BF}_4)_7\text{Cl} \cdot 2\text{CH}_3\text{CN} \cdot 2\text{H}_2\text{O}$

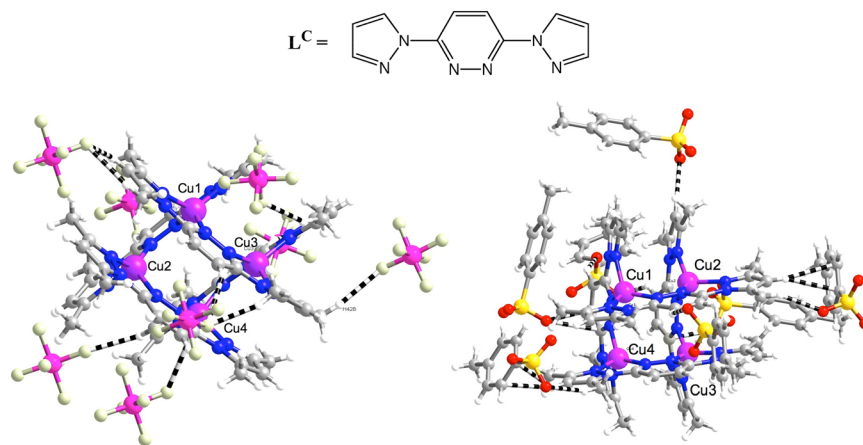


Fig. 3 Perspective views of the complicated arrays of weak interactions found in (left) $[\text{Cu}_4(\text{L}^{\text{C}})_4](\text{PF}_6)_4$ and (right) $[\text{Cu}_4(\text{L}^{\text{C}})_4](\text{CH}_3\text{C}_6\text{H}_4\text{SO}_3)_4$, both²¹ associated with a complete loss of grid symmetry.



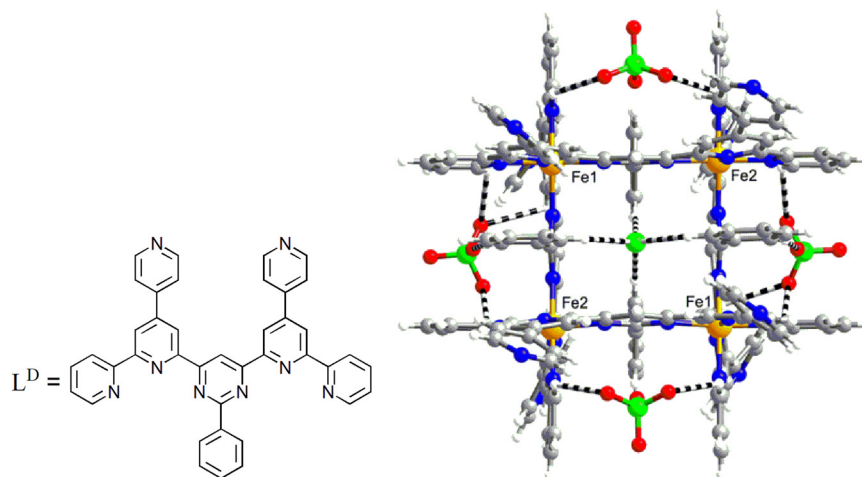


Fig. 4 Possible anion...grid interactions in the crystal³⁶ of $[\text{Fe}_4(\text{L}^D)_4]\text{Cl}(\text{ClO}_4)_7 \cdot 7\text{CH}_3\text{NO}_2 \cdot 6\text{H}_2\text{O}$. For clarity, disorder of pyridine groups is not shown.

(Fig. 5(b); CCDC 213092; refcode IYUBEJ),³⁸ where partial disorder of the $[\text{BF}_4]^-$ anions and lack of OH hydrogen locations limit complete analysis of H-bonding interactions but do not concern that of chloride interactions. The Hirshfeld surface of the chloride ion shows it to be

involved in two pairs of $\text{CH} \cdots \text{Cl}$ interactions at 2.54 and 2.73 Å and one pair of $\text{F} \cdots \text{Cl}$ interactions (involving ordered $[\text{BF}_4]^-$ anions) at 2.93 Å. The ligand units are tilted by near 110° to the Fe_4L_4 mean plane in such a way that the substituent OH groups of the pyrimidine core project

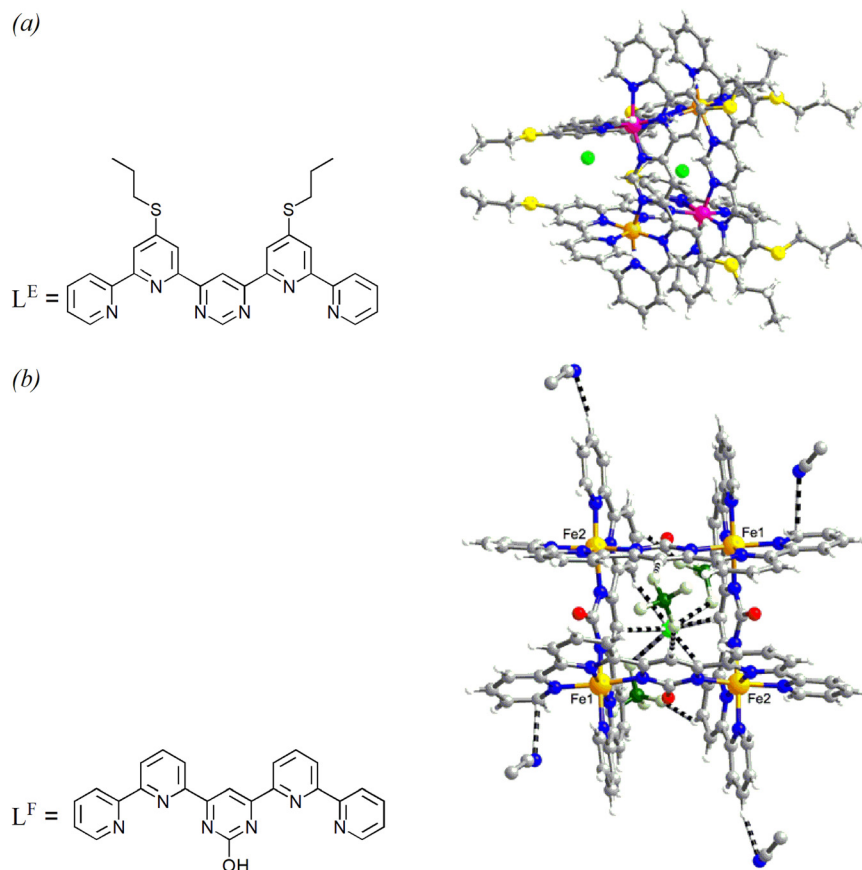


Fig. 5 (a) Perspective view of the positioning of chloride ions (green spheres) included in the grid found in the crystal³⁷ of $[\text{Fe}_2\text{Ru}_2(\text{L}^E)_4]\text{Cl}_2(\text{PF}_6)_2 \cdot 3\text{CH}_3\text{CN}$. Extensive disorder of this structure is not shown. (b) Identified weak interactions of ordered species in the grid present in the structure of the crystal³⁸ of $[\text{Fe}_4(\text{L}^F)_4](\text{BF}_4)_7\text{Cl} \cdot 2\text{CH}_3\text{CN} \cdot 2\text{H}_2\text{O}$.



outwards, with the O-atom possibly involved in interactions with adjacent N and C atoms of inner pyridine rings of orthogonal ligand units, although as all these atoms lie within the Hirshfeld surface, any interactions are not apparent on it. As the OH hydrogen was not located, its interactions cannot be defined but no H-bond acceptor atoms are present within <3.5 Å. Interactions of the grid with four ordered acetonitrile molecules all involve N but two are $N\cdots HC$ (terminal pyridine) and two $N\cdots C$ (terminal pyridine). With all ordered interactions considered, the grid aggregate has twofold rotational symmetry and thus two inequivalent Fe centres (Fig. 5(b)).

The tendency seen in both these structures of anions binding in a manner such that they form caps to the central cavity rather than entering within it is also seen in the structure of $[Cu_4(L^G)_4](PF_6)_4 \cdot H_2O \cdot 0.5CH_3OH$ (Fig. 6(a); CCDC 290965; refcode YENRUF),³⁹ a structure where the only deficiency is the lack of water hydrogen atom locations. Here, $[PF_6]^-$ anions are poised above and below the mean Cu_4 plane, one involved in just a single $F\cdots HC$ (pyrimidine) interaction with the grid core (plus two $F\cdots HC$ interactions with an adjacent grid and one apparent $F\cdots HO$ H-bond), the other involved in two $F\cdots HC$ (pyrimidine) and one

$F\cdots C$ (pyrimidine) interactions along with an $F\cdots HC$ (methanol) interaction and both $F\cdots H$ and $F\cdots C$ interactions with an adjacent grid. Although it is important to note in this and all other cases that a crystal can involve extended interactions which bridge individual components, it is assumed that proximity must determine the extent of influence of weak interactions on structure, and in YENRUF the unsymmetrical binding and positioning of the two anions removes all symmetry from their aggregate with the grid, explaining why all four Cu atoms are inequivalent centres (Fig. 6(a)). In contrast, in the grid $[Fe_4(L^H)_4](BF_4)_4 \cdot 2CH_3CN \cdot H_2O$ (CCDC 951971; refcode TIKXUI),⁴⁰ interactions of the anions with the grid involve exclusively $F\cdots H$ contacts (1.92 Å to NH and 2.27 Å to CH) that are such that the aggregate is centrosymmetric and all four $Fe(III)$ centres are equivalent (Fig. 6(b)). Neither acetonitrile nor water molecules are found in the grid cavity and their positioning does not seem to perturb this symmetry, though the lack of H-atom coordinates for both prevents clear assignment of their interactions.

One important step in developing simple and rapid syntheses of bis(tridentate) ligands suitable for grid formation with octahedral metal ions was based on

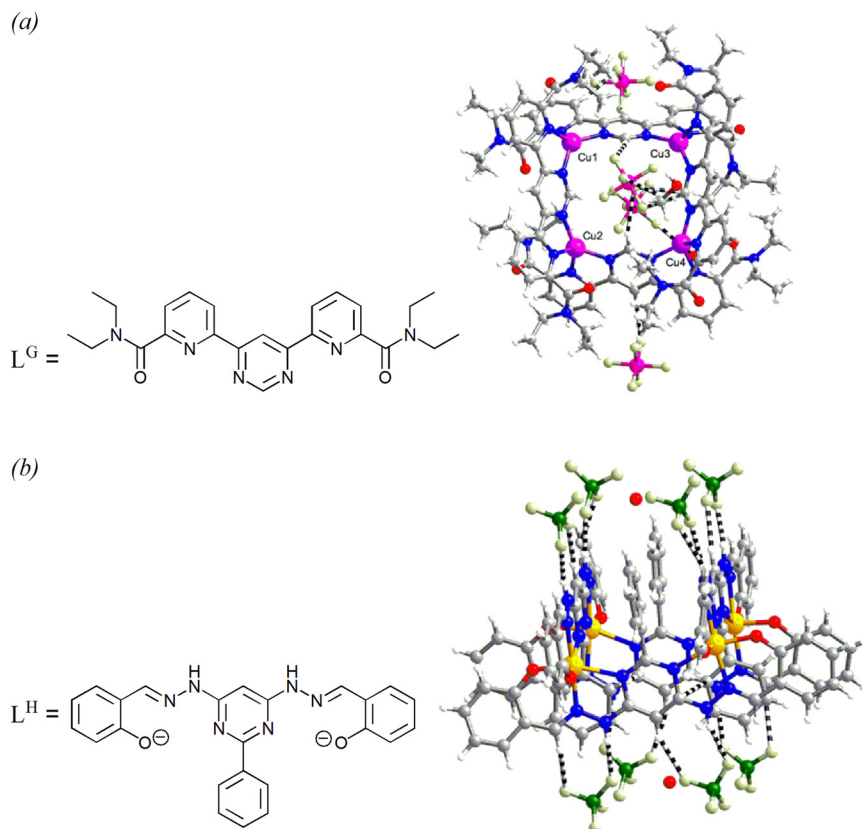


Fig. 6 (a) Weak interactions of the grid with its counteranions found in the crystal³⁹ of $[Cu_4(L^G)_4](PF_6)_4 \cdot H_2O \cdot 0.5CH_3OH$, showing capping of the central cavity by the anions. (b) Weak interactions of the anions with the grid in the crystal⁴⁰ of $[Fe_4(L^H)_4](BF_4)_4 \cdot 2CH_3CN \cdot H_2O$. Water molecules (isolated red spheres for their O-atoms) form plugs to the central cavity and are within H-bonding distances of tetrafluoroborate O-atoms but the H-atoms were not located.



recognition of the facility with which terpyridine analogues could be prepared through hydrazone formation reactions.⁴¹ For pyrimidine-core ligands, pyrimidine-4,6-dialdehyde and (less frequently) 4,6-dihydrazinopyrimidine (and their 2-phenyl derivatives)⁴² thus became starting materials for the syntheses of a large variety of metallogrids,^{3,6–8} though other hydrazone-based ligands have also been the basis of a very large family.^{2,5} Of the pyrimidine family, three closely

related Zn(II) grids for which structures involving minimal complications are available⁴³ have the compositions $[\text{Zn}_4(\text{L}^{\text{I}})_4](\text{O}_3\text{SCF}_3)_8 \cdot 8\text{CH}_3\text{CN}$ (Fig. 7(a); CCDC 288070; refcode VEDJIY), $[\text{Zn}_4(\text{L}^{\text{J}})_4](\text{O}_3\text{SCF}_3)_8 \cdot 4\text{CH}_3\text{CN} \cdot 4\text{H}_2\text{O}$ (Fig. 7(b); CCDC 288071; refcode VEDJOE), $[\text{Zn}_4(\text{L}^{\text{K}})_4](\text{O}_3\text{SCF}_3)_8 \cdot 6\text{CH}_3\text{CN} \cdot (\text{C}_6\text{H}_6)_{1.5} \cdot \text{C}_2\text{H}_5\text{OH} \cdot 2\text{H}_2\text{O}$ (Fig. 7(c); CCDC 288072; refcode VEDJUK). VEDJIY is a structure free of any disorder where the Hirshfeld surface shows weak interactions with the grid

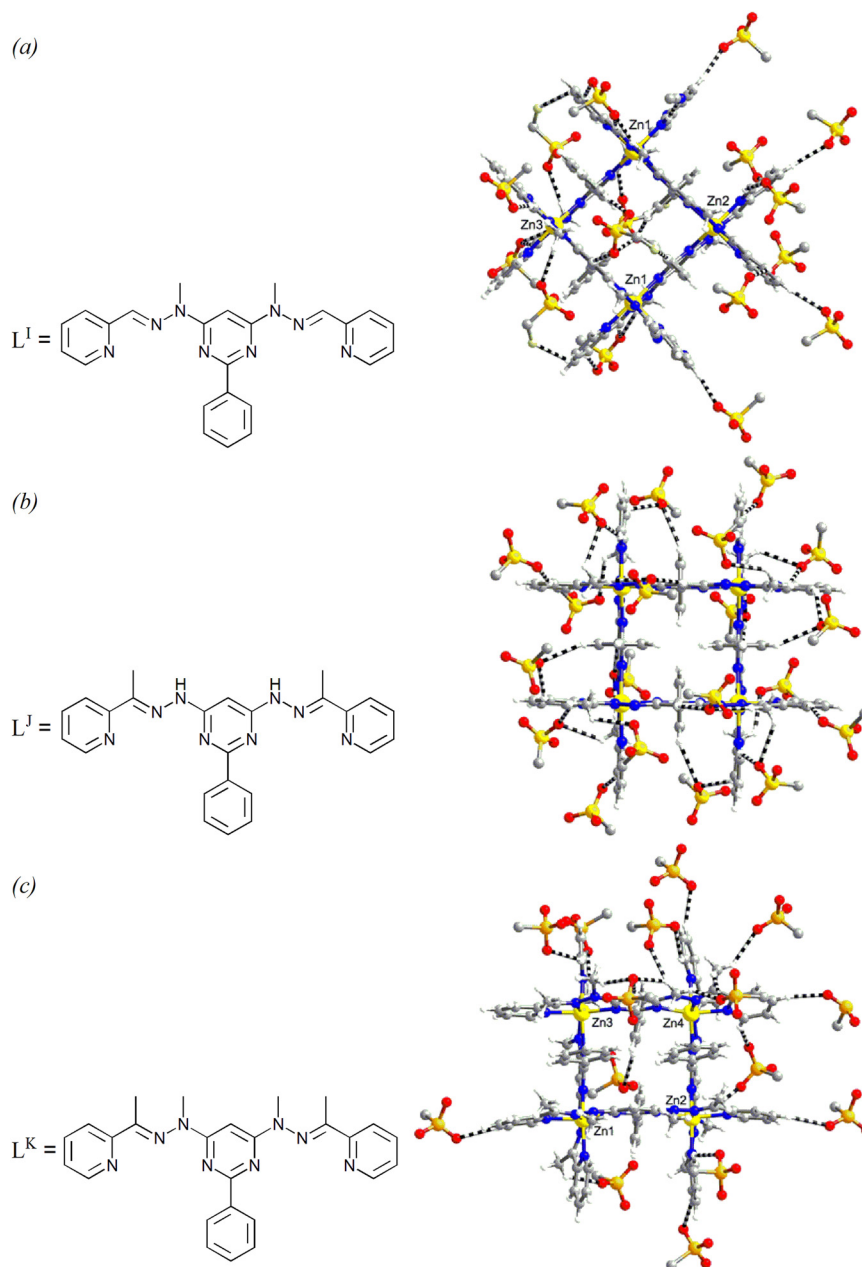


Fig. 7 (a) Grid···anion interactions found in the crystals⁴³ of $[\text{Zn}_4(\text{L}^{\text{I}})_4](\text{O}_3\text{SCF}_3)_8 \cdot 8\text{CH}_3\text{CN}$, showing the twofold rotational symmetry of the aggregate. For clarity, triflate F-atoms are not shown except for the four involved in F···H(aromatic) contacts (two at 2.58 and two at 2.62 Å). (b) Grid···anion interactions in the crystals⁴³ of $[\text{Zn}_4(\text{L}^{\text{J}})_4](\text{O}_3\text{SCF}_3)_8 \cdot 4\text{CH}_3\text{CN} \cdot 4\text{H}_2\text{O}$, a complicated array involving both O···HC(aromatic) and O···HC(aliphatic) contacts of fourfold symmetry, meaning all four Zn centres are equivalent. Triflate F-atoms are not shown. (c) Similar grid···anion interactions in the crystals⁴³ of $[\text{Zn}_4(\text{L}^{\text{K}})_4](\text{O}_3\text{SCF}_3)_8 \cdot 6\text{CH}_3\text{CN} \cdot (\text{C}_6\text{H}_6)_{1.5} \cdot \text{C}_2\text{H}_5\text{OH} \cdot 2\text{H}_2\text{O}$ but here lacking all symmetry, so that the four Zn centres are inequivalent. Triflate F-atoms are not shown.



unit to involve O \cdots HC(aromatic and aliphatic) contacts with sixteen triflate oxygen atoms, two F \cdots HC(aromatic) contacts with fluorine from two of the sixteen triflates and four N \cdots HC(aromatic) contacts from acetonitrile molecules. The array produced is such that a C₂ symmetry axis passes along one ZnZn diagonal but not along the other, so that there are three inequivalent Zn centres in the grid (Fig. 7(a)). In VEDJOE, there is disorder of the fluorine atoms of half the triflate anions but the Hirshfeld surface provides no indication of grid-fluorine contacts, only of eight apparent O \cdots N(hydrazone) interactions which are presumably H-bonds involving the unlocated NH group, and twelve ordered-O \cdots HC(aromatic and aliphatic) interactions of triflate anions, plus (nitrile)C \cdots C(aromatic) interactions involving eight acetonitrile molecules. About each Zn ion the array is the same, so this is a case where all four Zn centres are equivalent in the grid in the crystal state (Fig. 7(b)). In VEDJUK, despite the several quite different solvents present in the crystal, none is found in the central cavity and interactions with the grid are dominated by those with triflate anions in an unsymmetrical array making all Zn centres inequivalent (Fig. 7(c)).

An illustration of the sophisticated decoration of a grid attainable through the use of hydrazone-based ligands, designed with the objective of obtaining multivalent receptors, can be found in the complex [Cu₄(L^L)₄](BF₄)₈·10.5CH₃CN·4.5C₇H₈ (Fig. 8; CCDC 711187; refcode GUGTAE).⁴⁴ The structure here suffers only a lack of H-atom coordinates for some of the acetonitrile and solvent molecules and all interactions beyond dispersion with the grid units are well defined on the Hirshfeld surface. No species occupy the mean plane of the Cu₄ group but tetrafluoroborate anions lie above each side of this plane and are involved in multiple F \cdots HC interactions in an array which removes all symmetry, consistent with all four Cu centres being inequivalent. Interactions with three acetonitrile molecules involving both N \cdots HC and (methyl)H \cdots O contacts are also unsymmetrical (Fig. 8).

Several of the structures referred to so far involve bisolvated crystals, raising the issue of selectivity of solvent interactions in determining solubility. There is of course no guarantee that what may be seen in the crystal reflects what is occurring in solution, where the ratio grid:solvent(s) may be very different. In essentially all known instances, the solvents present in grid complex crystals have been determined by the choice deemed appropriate to obtain crystals suitable for X-ray structure determinations, not by a choice for investigation of solvate selectivity. Acetonitrile has been commonly used as a solvent for grid complexes and for this reason is found in several of the crystal structures discussed above but nitromethane has also been commonly employed and an example of its (bi)solvate formation may be found in the complex [Mn₄(L^M)₄](ClO₄)₈·12CH₃NO₂·7H₂O (Fig. 9; CCDC 207377; refcode BARYUP).⁴⁵ Its structure is free of disorder except for some of the perchlorate anions and although H-atom coordinates are not available for the water molecules, interactions of nitromethane with the grid can be defined through the Hirshfeld surface. Neither water nor nitromethane is found in the central cavity of the grid and although seven nitromethane molecules can be considered associated with each grid unit, two appear to be held by dispersion forces only and five are involved in interactions (four O \cdots HC and one O \cdots C) with rather long atom separations, indicating them to be particularly weak. Seven of the hydrazone NH atoms are involved in rather short H-bond interactions with water molecules, while the eighth forms a charge-assisted H-bond to perchlorate-O. Eight perchlorate units, both ordered and disordered, are involved in O \cdots HC(aromatic) interactions mainly about the periphery of the grid and the total array of anion and solvent interactions has no symmetry, consistent with the fact that all four Mn centres are inequivalent (Fig. 9). In terms of their locations in the crystals, there is certainly some selectivity shown for the solvents but this results from different interaction modes and it must be said that

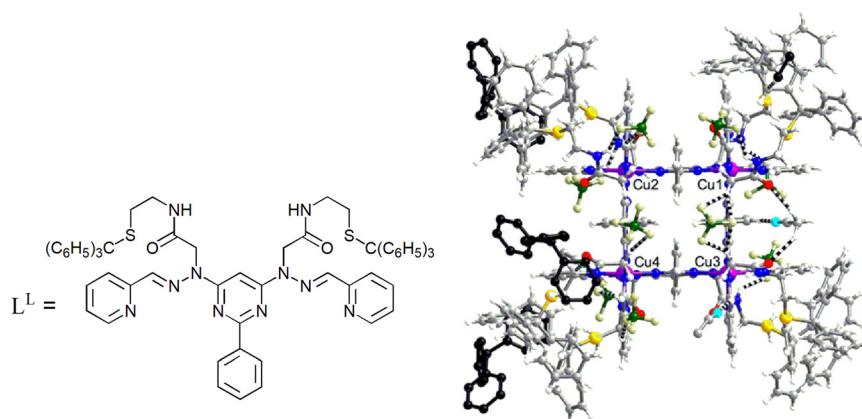


Fig. 8 Grid interactions involving [BF₄]⁻ anions, CH₃CN solvent and adjacent grid units in the crystals⁴⁴ of [Cu₄(L^L)₄](BF₄)₈·10.5CH₃CN·4.5C₇H₈. Solvent N-atoms are shown in light blue and atoms of adjacent grid units in black. The grid has no symmetry.



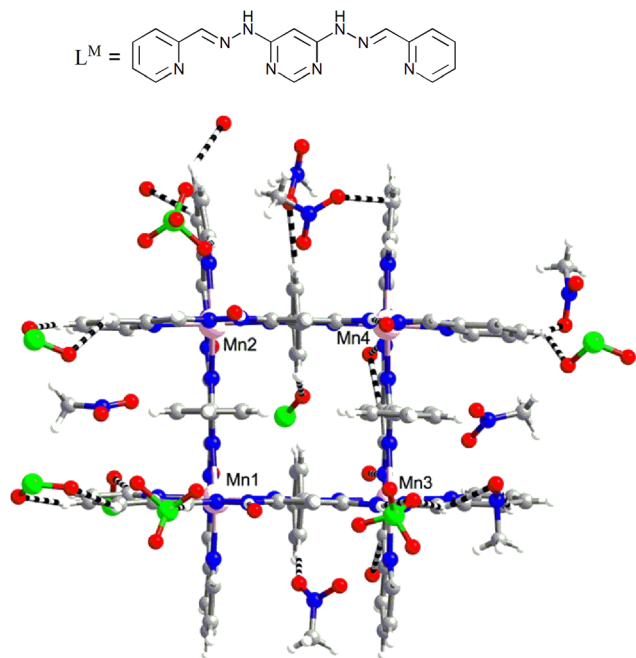


Fig. 9 Grid interactions involving anions and solvents in the crystal⁴⁵ of $[\text{Mn}_4(\text{L}^{\text{M}})_4](\text{ClO}_4)_8 \cdot 12\text{CH}_3\text{NO}_2 \cdot 7\text{H}_2\text{O}$. Water O-atoms involved in H-bond acceptance from hydrazone NH and aromatic CH are shown as isolated red spheres, and two nitromethane molecules appear to be held in position by dispersion forces only. The array has no symmetry. Disordered perchlorate anions are shown without their full complement of O-atoms.

the presence of both solvents is important in ensuring that the species actually crystallised is the least soluble of all that might be possible.

One means of reducing the symmetry of homometallic grids is to use unsymmetrical ligands and an elegant example of this approach can be found in the covalent linking of two ditopic ligands into a linear tetratopic ligand L^{N} which has a plane of symmetry but has inequivalent “inner” and “outer” coordination sites.⁹ Thus, the complex $[\text{Zn}_4(\text{L}^{\text{N}})_2](\text{O}_3\text{SCF}_3)_8 \cdot 2\text{H}_2\text{O} \cdot 2\text{CH}_3\text{CN}$ (Fig. 10(a); CCDC 2087825; refcode ODAQOD),⁹ as a result of the linking of two ditopic units, can have no higher than C_2 symmetry and this is observed to be the case, with three inequivalent Zn centres making up the grid. Weak interactions of the grid, which involve not only acetonitrile- $\text{N} \cdots \text{C}$, triflate- $\text{O} \cdots \text{HC}$, triflate- $\text{O} \cdots \text{C}$ and triflate- $\text{F} \cdots \text{HC}$ contacts but also $\text{O} \cdots \text{HC}$ and $\text{C} \cdots \text{HC}$ contacts with adjacent ligand units, do not perturb this symmetry (Fig. 10(a)). In the case of the complex $[\text{Zn}_4(\text{L}^{\text{O}})_2](\text{O}_3\text{SCF}_3)_8$ (Fig. 10(b); CCDC 2087824; refcode ODAWOJ),⁹ where L^{O} is a symmetrical tetratopic macrocycle that might be expected to form a grid with all four metal centres being equivalent, however, weak interactions do have an effect and again there are three inequivalent Zn centres (in a grid unit of C_2 symmetry; Fig. 10(b)). The interactions are largely due to triflate- $\text{O} \cdots \text{HC}$ and triflate- $\text{O} \cdots \text{C}$ contacts but again there are some interactions ($\text{O} \cdots \text{HC}$ and $\text{CH} \cdots \text{O}$) with adjacent grids. In this structure, there is some disorder of the pyridine rings

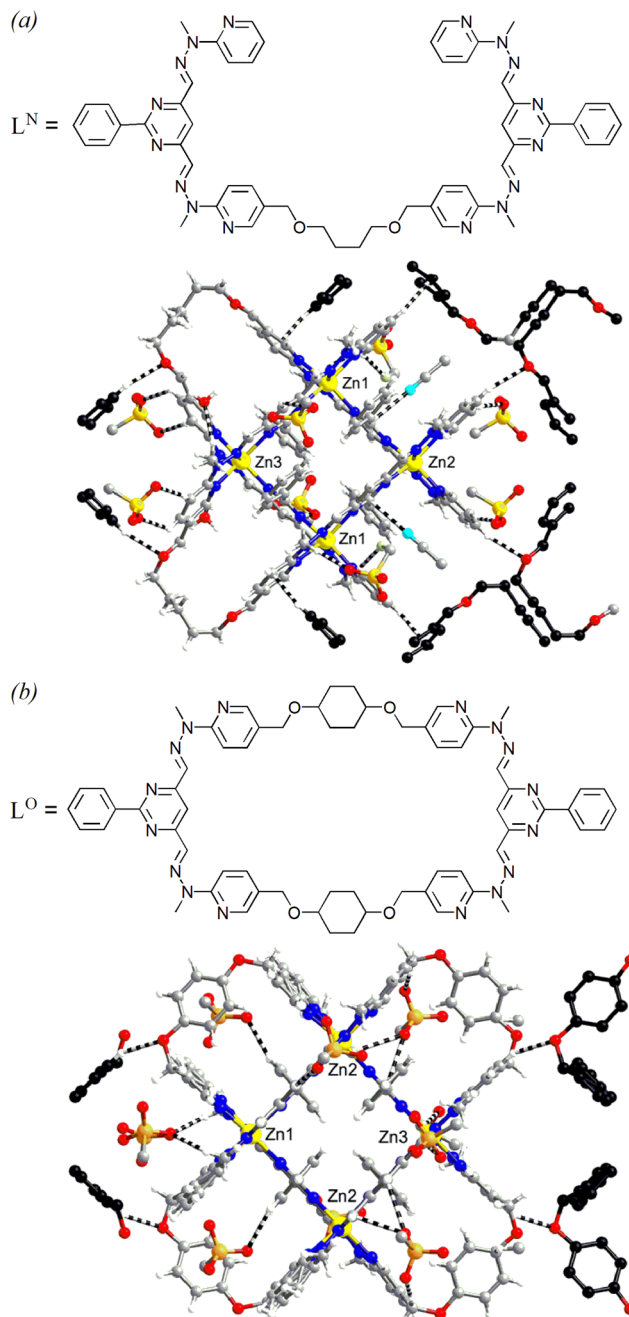


Fig. 10 (a) Interactions of the grid present in the crystal⁹ of $[\text{Zn}_4(\text{L}^{\text{N}})_2](\text{O}_3\text{SCF}_3)_8 \cdot 2\text{H}_2\text{O} \cdot 2\text{CH}_3\text{CN}$ involving not only the anions and both solvents but also, again, adjacent grids. Acetonitrile-N is shown in light blue and C-atoms of adjacent grids in black. The aggregate has twofold rotational symmetry about the $\text{Zn}_2\text{-Zn}_3$ axis. Triflate F-atoms are not shown. (b) Interactions of the grid present in the partly disordered crystal⁹ of $[\text{Zn}_4(\text{L}^{\text{O}})_2](\text{O}_3\text{SCF}_3)_8$, where again there are some direct interactions with adjacent grids. Triflate F-atoms are not shown.

which renders assignment of apparent triflate- O interactions uncertain, so for clarity these are not shown.

The grids discussed above are all cationic, so it would be expected that charge influences would favour close association with anions which might exclude neutral molecules from the vicinity of the grids, regardless of the



nature of the weak interactions involved in the association with either species.⁴⁶ There are many ways of obtaining neutral grids^{2–8,17,47} and even ways of decorating neutral grids with charge-bearing substituents so that charge centres are remote from the neutral core⁴⁸ but obviously simple neutral grids would be the reference species for investigation of neutral molecule inclusion. Structural studies¹⁷ of neutral grids obtained from acylhydrazones of 2-phenylpyrimidine-4,6-dialdehyde (after deprotonation) have shown that the crystals commonly contain highly hydrated grids but only in one case (Fig. 11; CCDC 637563; refcode OFEDOT; $[\text{Cu}_4(\text{L}^{\text{P}})_4]\cdot 2\text{H}_2\text{O}$), a Cu(II) grid where the acyl group is octanoyl, have water hydrogen atoms been located. The Hirshfeld surface for this crystal, where there is a relatively low degree of hydration, shows that interactions of water molecules with the grid involve “classical” $\text{OH}\cdots\text{O}(\text{acyl})$ and $\text{OH}\cdots\text{N}(\text{hydrazonyl})$ hydrogen bonding with two opposed Cu centres being involved in the former while the other two are involved in the latter. This differentiation is consistent with the fact that there are two inequivalent Cu sites within the grid, each equivalent pair being related by a twofold rotation axis perpendicular to the Cu_4 mean plane. (Fig. 11). If the $\text{O}\cdots\text{O}$ and $\text{O}\cdots\text{N}$ distances for H-bonds found in this structure are presumed to provide values ($<3 \text{ \AA}$) applicable to the structures in which H coordinates of the water molecules are missing, then it is possible to assign water H-bonding interactions in all of the studied structures and the

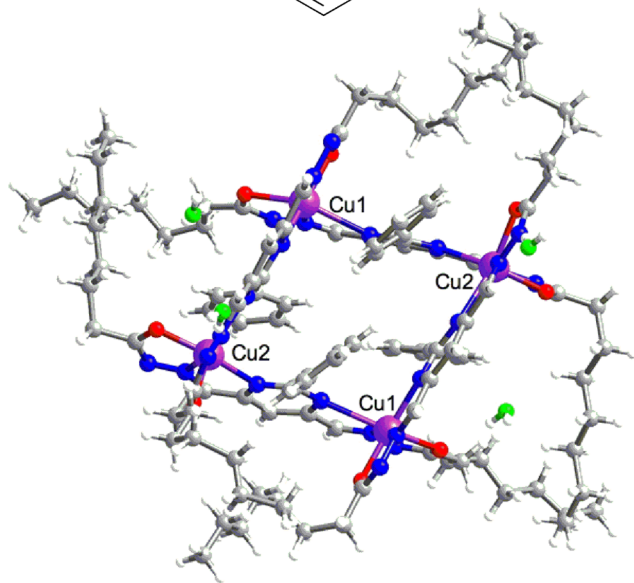
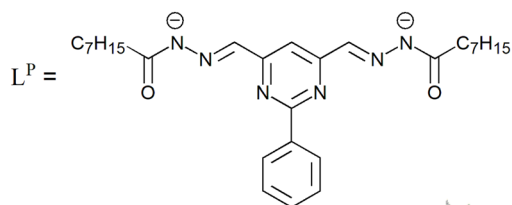


Fig. 11 “Classical” H-bonding interactions of water with the grid present in the crystal¹⁷ of $[\text{Cu}_4(\text{L}^{\text{P}})_4]\cdot 2\text{H}_2\text{O}$. Water molecule O-atoms are shown in green. Water– $\text{O}\cdots\text{O}(\text{ligand})$ 2.87, water– $\text{O}\cdots\text{N}(\text{ligand})$ 2.92 Å.

aggregates thereby defined have the symmetry giving the different numbers of inequivalent metal ion sites seen in these structures (Fig. S3(i)–(vii)). In no case is water found to be included in the central grid cavity and while this may be a simple consequence of a preference for interaction at H-bond acceptor sites (including other water molecules not in direct interaction with the grid) elsewhere, it is well known that water can be included within hydrophobic cavities such as those of calixarenes⁴⁹ and cyclodextrins,⁵⁰ so that water molecule interactions with simple phenyl groups near the grid core are possibly too weak to cause inclusion.

Conclusions

The analysis of weak interactions in crystalline solids is complicated by the very fact that their weakness often leads to ill-defined composition or the presence of electron density of molecularly unassignable nature (disposed of by the SQUEEZE⁵¹ technique) but more often that any molecule of moderate size may have several sites where weak interactions can occur and the sites actually involved in any given crystal structure can vary. This is seen in the cases discussed herein for acetonitrile, formally present as a solvate molecule, where interactions involve $\text{N}\cdots\text{HC}$, $(\text{methyl})\text{CH}\cdots\text{O}$ and $(\text{nitrile})\text{C}\cdots\text{C}(\text{aromatic})$ contacts, sometimes but not always together. It also arises with fluoroanions such as $[\text{BF}_4]^-$ and $[\text{PF}_6]^-$, where both $\text{F}\cdots\text{H}$ and $\text{F}\cdots\text{C}(\text{aromatic})$ interactions with grids occur in various patterns. Weak interactions are labile interactions, so the form of any solvate crystal is not necessarily a reflection of the dominant species in its mother liquor, and recognising that dispersion forces play a significant role in the assembly of any crystal, it is far from straightforward to draw any conclusions regarding binding selectivity in solvate formation from a crystal structure alone. It is of course possible to perform high-level computational modelling (and CrystalExplorer,²⁹ for example, can be augmented to do exactly just that) to evaluate the energy of all particular interactions but for a whole crystal this remains a demanding procedure with its own limitations.⁵² The utility of Hirshfeld surface analysis at its basic level as applied in the present work is that it provides models of how weak interactions are mediated as atom contacts and, more importantly, that it provides evidence that weak interactions do have a significant influence on the symmetry of the host species. Grids based on paramagnetic metal ions such as Cu(II) constitute an array of spins and thus might find application in quantum information science,²⁵ though presumably any site equivalences within the grid would be important.

Concerning the possibility of grids acting as neutral molecule receptors, it is clear that use of ligands based on a pyrimidine core generates a rather small cavity, often capped when the grid is cationic by counter anions like $[\text{BF}_4]^-$ and $[\text{ClO}_4]^-$,^{38,39,53} but the fact that it is unoccupied in all the systems discussed herein cannot be taken to mean that inclusion there is impossible because the available structures



of solvate species involve only polar solvents (or one moderately large apolar species) capable of strongly interacting with other parts of the grids. What is clear from even just the presently considered examples, nonetheless, is that atoms within the pyrimidine units do undergo weak interactions of different forms involving at least aromatic-CH and ring carbon centres. It would obviously be of interest to further extend studies²⁴ of the inclusion of CO₂ by grids, especially given that the better of the known examples was a neutral, unsolvated species, and to investigate the binding of other small potential guests such as N₂O, NO and CO.

Conflicts of interest

There are no conflicts of interest to declare.

Data availability

The software used for structural analysis is CrystalExplorer,²⁹ a program for Hirshfeld surface analysis, visualization and quantitative analysis of molecular crystals. CrystalExplorer is accessible from <https://crystalexplorer.net/>.

Their numbers/refcodes are: 162905/TIWCOS; 681835/TIWCUY; 681836/TIWDAF; 681837/TIWDEJ; 681838/TIWDIN; 123202/RUHXUN; 279772/MAYXEQ; 238750/FEKRET; 101633/SIQPIR; 213092/IYUBEJ; 290965/YENRUF; 951971/TIKXUI; 288070/VEDJIY; 288071/VEDJOE; 288072/VEDJUK; 711187/GUGTAE; 207377/BARYUP; 2087825/ODAQOD; 2087824/ODAWOJ; 637563/OFEDOT.

Supplementary information (SI): Hirshfeld surface diagrams for the grid units, analysis of the Hirshfeld surfaces, and representations of the hydrogen bonding in neutral grid hydrates referred to in the main text. See DOI: <https://doi.org/10.1039/d6ce00269b>.

References

- For self-organization by design, see: (a) J.-M. Lehn, *Angew. Chem., Int. Ed. Engl.*, 1988, **27**, 89–112; (b) J.-M. Lehn, *Science*, 2002, **295**, 2400–2403; (c) J.-M. Lehn, *Proc. Natl. Acad. Sci. U. S. A.*, 2002, **99**, 4763–4768; (d) J.-M. Lehn, *Chem. Soc. Rev.*, 2007, **36**, 151–160; (e) J.-F. Ayme and J.-M. Lehn, *Adv. Inorg. Chem.*, 2018, **71**, 3–69; (f) J.-M. Lehn, *Isr. J. Chem.*, 2018, **58**, 136–141.
- L. K. Thompson, *Coord. Chem. Rev.*, 2002, **233–234**, 193–206.
- M. Ruben, J. Rojo, F. J. Romero-Salguero, L. H. Uppadine and J.-M. Lehn, *Angew. Chem.*, 2004, **116**, 3728–3747.
- L. N. Dawe, T. S. M. Abedin and L. K. Thompson, *Dalton Trans.*, 2008, 1661–1675.
- L. N. Dawe, K. V. Shuvaev and L. K. Thompson, *Chem. Soc. Rev.*, 2009, **38**, 2334–2359.
- A.-M. Stadler, *Eur. J. Inorg. Chem.*, 2009, 4751–4770.
- J. G. Hardy, *Chem. Soc. Rev.*, 2013, **42**, 7881–7899.
- Q. Yang and J. Tang, *Dalton Trans.*, 2019, **48**, 769–778.
- J. Holub, A. Santoro, A.-M. Stadler and J.-M. Lehn, *Inorg. Chem. Front.*, 2021, **8**, 5054–5064.
- M. Ruben, J. Rojo, F. J. Romero-Salguero, L. H. Uppadine and J.-M. Lehn, *Angew. Chem., Int. Ed.*, 2004, **43**, 3644–3662.
- K. S. Kumar and M. Ruben, *Coord. Chem. Rev.*, 2017, **346**, 176–205.
- J. Holub, A. Santoro and J.-M. Lehn, *Inorg. Chim. Acta*, 2019, **494**, 223–231.
- M. Ruben, J.-M. Lehn and P. Müller, *Chem. Soc. Rev.*, 2006, **35**, 1056–1067.
- C. Romeike, M. R. Wegewijs, M. Ruben, W. Wenzel and H. Schoeller, *Phys. Rev. B: Condens. Matter Mater. Phys.*, 2007, **75**, 064404.
- M. A. Naumova, A. Kalinko, J. W. L. Wong, S. A. Gutierrez, J. Meng, M. Liang, M. Abdellah, H. Geng, W. Lin, K. Kubicek, M. Biednov, F. Lima, A. Galler, P. Zalden, S. Checchia, P.-A. Mante, J. Zimara, D. Schwarzer, S. Demeshko, V. Murzin, D. Gosztola, M. Jarenmark, J. Zhang, M. Bauer, M. L. L. Daku, D. Khakhulin, W. Gawelda, C. Bressler, F. Meyer, K. Zheng and S. E. Canton, *J. Chem. Phys.*, 2020, **152**, 214301.
- F. Nachon, X. Brazzalotto, J. Dias, C. Courageux, W. Drozd, X.-Y. Cao, A. R. Stefankiewicz and J.-M. Lehn, *ChemBioChem*, 2022, **23**, e202200456.
- X.-Y. Cao, J. Harrowfield, J. Nitschke, J. Ramirez, A.-M. Stadler, N. Kyritsakas-Gruber, A. Madalan, K. Rissanen, L. Russo, G. Vaughan and J.-M. Lehn, *Eur. J. Inorg. Chem.*, 2007, 2944–2965.
- D. H. Busch, *Top. Curr. Chem.*, 2004, **249**, 1–65.
- D. Zhang, T. K. Ronson and J. R. Nitschke, *Acc. Chem. Res.*, 2018, **51**, 2423–2436.
- A. Milo, N. S. Sigman and E. N. Jacobsen, *Chem. Rev.*, 2025, **125**, 9089–9091.
- B. R. Manzano, F. A. Jalón, I. M. Ortiz, M. L. Soriano, F. Gómez de la Torre, J. Elguero, M. A. Maestro, K. Mereiter and T. D. W. Claridge, *Inorg. Chem.*, 2008, **47**, 413–428.
- C. S. Campos-Fernández, B. L. Schottel, H. T. Chifotides, J. K. Bera, J. Bacsá, J. M. Koomen, D. H. Russell and K. R. Dunbar, *J. Am. Chem. Soc.*, 2005, **127**, 12909–12923.
- H. T. Chifotides, I. D. Giles and K. R. Dunbar, *J. Am. Chem. Soc.*, 2013, **135**, 3039–3055.
- M. Sooraj, R. Jayakrishnan and E. Manoj, *Dalton Trans.*, 2025, **54**, 6922–6934.
- G. D. Scholes, A. Olaya-Castro, S. Mukamel, A. Kirrander, K.-K. Ni, G. J. Hedley and N. L. Frank, *J. Phys. Chem. Lett.*, 2025, **16**, 1376–1396.
- F. le Madelé, I. Mohelsky, J. Wyzula, M. Orliá, P. Turek, F. Trolani and A. K. Boudalis, *Nat. Commun.*, 2025, **16**, 1198.
- A. S. Batsanov, *Acta Crystallogr., Sect. E: Crystallogr. Commun.*, 2018, **74**, 570–574.
- M. A. Spackman and D. Jayatilaka, *CrystEngComm*, 2009, **11**, 19–32.
- P. R. Spackman, M. J. Turner, J. J. McKinnon, S. K. Wolff, D. J. Grimwood, D. Jayatilaka and M. A. Spackman, *J. Appl. Crystallogr.*, 2021, **54**, 1006–1011.
- Interesting “alternate” (for a recent example, see (a) E. Day, B. Kauffmann, M. Scarpi-Luttenuer, A. Chaumont, M.



- Henry and P. Mobian, *Chem. – Eur. J.*, 2022, **19**, e202200047; see also the references therein) and “cross” (for a recent example, see (b) M. K. Thangavel, J. Harrowfield, C. Bailly, L. Karmazin and A.-M. Stadler, *Dalton Trans.*, 2022, **51**, 14107–14117; see also the references therein) [2×2] grids, which contain ditopic ligands with oppositely oriented coordination sites, are not discussed here.
- 31 M.-T. Youinou, N. Rahmouni, J. Fischer and J. A. Osborn, *Angew. Chem., Int. Ed. Engl.*, 1992, **31**, 733–735.
- 32 P. J. Bettle, L. N. Dawe, M. U. Anwar and L. K. Thompson, *Eur. J. Inorg. Chem.*, 2011, 5036–5042.
- 33 P. N. W. Baxter, J.-M. Lehn, B. O. Kneisel and D. Fenske, *Chem. Commun.*, 1997, 2231–2232.
- 34 T. S. M. Abedin, L. K. Thompson and D. O. Miller, *Chem. Commun.*, 2005, 5512–5514.
- 35 J. Rojo, F. J. Romero-Salguero, J.-M. Lehn, G. Baum and D. Fenske, *Eur. J. Inorg. Chem.*, 1999, 1421–1428.
- 36 M. Ruben, U. Ziener, J.-M. Lehn, V. Ksenofontov, P. Gütllich and G. B. M. Vaughan, *Chem. – Eur. J.*, 2004, **11**, 94–100.
- 37 D. M. Bassani, J.-M. Lehn, K. Fromm and D. Fenske, *Angew. Chem., Int. Ed.*, 1998, **37**, 2364–2367.
- 38 M. Ruben, E. Breuning, J.-M. Lehn, V. Ksenofontov, P. Gutlich and G. Vaughan, *J. Magn. Magn. Mater.*, 2004, **272**, e715.
- 39 V. Patroniak, J.-M. Lehn, M. Kubicki, A. Ciesielski and M. Walesa, *Polyhedron*, 2006, **25**, 2643–2649.
- 40 A. R. Stefankiewicz, A. M. Madalan, J. M. Harrowfield and J.-M. Lehn, *CrystEngComm*, 2013, **15**, 9128–9134.
- 41 (a) J. F. Geldard and F. Lions, *J. Am. Chem. Soc.*, 1962, **84**, 2262–2263; (b) J. F. Geldard and F. Lions, *Inorg. Chem.*, 1963, **2**, 270–282.
- 42 J.-L. Schmitt, A.-M. Stadler, N. Kyritsakas and J.-M. Lehn, *Helv. Chim. Acta*, 2003, **86**, 1598–1624.
- 43 M. Barboiu, M. Ruben, G. Blasen, N. Kyritsakas, E. Chacko, M. Dutta, O. Radekovich, K. Lenton, D. J. R. Brook and J.-M. Lehn, *Eur. J. Inorg. Chem.*, 2006, 784–792.
- 44 A. R. Stefankiewicz, G. Rogez, J. M. Harrowfield, M. Drillon and J.-M. Lehn, *Dalton Trans.*, 2009, 5787–5802.
- 45 M. Ruben, J.-M. Lehn and G. Vaughan, *Chem. Commun.*, 2003, 1338–1339.
- 46 A. Gavezzotti, *CrystEngComm*, 2013, **15**, 4027–4035.
- 47 M. J. Chmielewski, E. Buhler, J. Candau and J. M. Lehn, *Chem. – Eur. J.*, 2014, **20**, 6960–6977.
- 48 W. Drozd, Y. Bessin, V. Gervais, X.-Y. Cao, J.-M. Lehn, A. R. Stefankiewicz and S. Ulrich, *Chem. – Eur. J.*, 2018, **24**, 1518–1521.
- 49 J. M. Notestein, A. Katz and E. Iglesia, *Langmuir*, 2006, **22**, 4004–4014.
- 50 S. Pereva, V. Nikolova, S. Angelova, T. Spassov and T. Dudev, *Beilstein J. Org. Chem.*, 2019, **15**, 1592–1600.
- 51 A. L. Spek, *Acta Crystallogr., Sect. C: Struct. Chem.*, 2015, **71**, 9–18.
- 52 M. Gao, D. G. Palmer and M. T. Dove, *MRS Commun.*, 2025, **15**, 1007–1016.
- 53 A. M. Madalan, X.-Y. Cao, G. Rogez and J.-M. Lehn, *Inorg. Chem.*, 2014, **53**, 4275–4277.

